AD-A139 984 EXPECTED ENERGY METHOD FOR ELECTRO-OPTICAL SNR CALCULATIONS(U) MASSACHUSETTS INST OF TECH LEXINGTON LINCOLN LAB G J MAYER 02 FEB 84 TR-634 ESD-TR-83-245 1/1

UNCLASSIFIED F19628-80-C-0002 F/G 12/1 NL

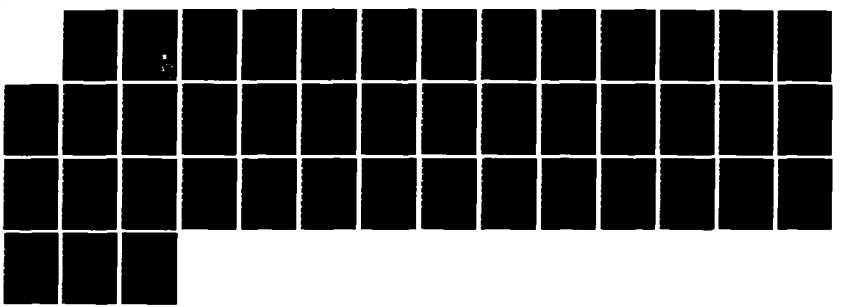

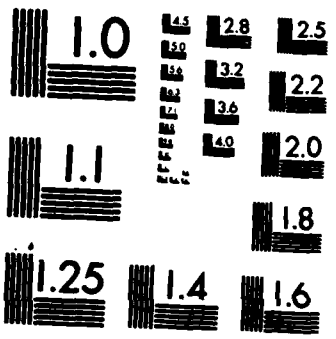

ESD-TR-83-245

Technical Report
634

Expected Energy Method for Electro-Optical SNR Calculations

G.J. Mayer

2 February 1984

Lincoln Laboratory
MASSACHUSETTS INSTITUTE OF TECHNOLOGY
LEXINGTON, MASSACHUSETTS

Prepared for the Department of the Air Force
under Electronic Systems Division Contract F19628-80-C-0002.

The work reported in this document was performed at Lincoln Laboratory, a center for research operated by Massachusetts Institute of Technology, with the support of the Department of the Air Force under Contract F19628-80-C-0002.

This technical report has been reviewed and is approved for publication.

FOR THE COMMANDER

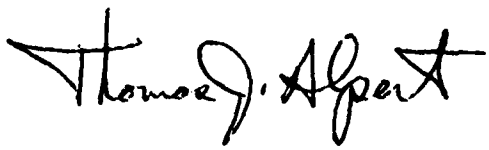

Thomas J. Alpert, Major, USAF
Chief, ESD Lincoln Laboratory Project Office

MASSACHUSETTS INSTITUTE OF TECHNOLOGY
LINCOLN LABORATORY

EXPECTED ENERGY METHOD FOR ELECTRO-OPTICAL SNR CALCULATIONS

G.J. MAYER

Group 94

TECHNICAL REPORT 634

2 FEBRUARY 1984

LEXINGTON **MASSACHUSETTS**

Abstract

A mathematically robust method is derived that allows the SNR of an electro-optical system to be estimated when a point source image falls onto a sensor array of discrete picture elements (pixel). The derivation is based on a geometrical analysis of image and sensor element configuration. This method allows the optimal pixel size to be selected to maximize the expected SNR for any point source image once it's diameter is known. In this report the method is used to determine the probability of an image falling into one, two, . . ., six pixels as a function of image diameter and pixel size, and the corresponding expected maximum signal. Examples are given using this method to estimate the SNR for an electro-optical system.

CONTENTS

I. INTRODUCTION

The analysis of the performance of an electro-optical system to detect point source images is greatly simplified by the assumption that the images each fall in one sensor array picture element[1] (pixel). This assumption is not valid when hundreds of star images and one or more unresolved satellite images (due to reflected sunlight) fall on a focal plane of thousands of pixels, because although some of the images will fall entirely in one pixel many will fall in two or more pixels. When an image falls in one pixel, the maximum electrical signal generated is proportional to the total image photons, but when an image falls in more than one pixel the maximum electrical signal becomes a function of the distribution of the image photons in the various pixels. One of the pixels will contain most of the image photons and will give the maximum electrical signal. The maximum electrical signal is of paramount importance because if the maximum signal crosses a threshold the image can be detected, but if the maximum signal fails to cross a threshold the image will not be detected. The maximum signal resulting from an image falling in several pixels would be less, sometimes twenty-five percent of the signal that would result if the image had fallen in one pixel, as will be shown in Section II. This decreased signal is the reason that predicted satellite detection performance and false alarm rates due to stars would be inaccurate if the simplified assumption that all images fall in one pixel is made.

Since the maximum signal is a function of the distribution of image photons in the various pixels; the number of pixels that an image occupies must first be determined, then the distribution of photons in those pixels

must be found. The maximum signal is due to the pixel with the most photons, therefore only the number of photons in this pixel have to be known.

The energy (number of image photons) collected by a pixel can be determined geometrically for any circular image diameter and pixel size by specifying the location of the image center. If the image falls randomly on the focal plane (no tracking of images), the probability distribution of image centers is uniform. When the image is confined to two pixels, the area that the image centers can occupy is limited and the distribution of image centers is uniform. The expected location of the image center is therefore the centroid of this area[3]. Once the expected image center location is determined the expected energy in each pixel can be uniquely determined. For the two pixel situation the expected energy in each pixel is 50 percent of the total. The method is deceptively simple for the cases of the image being in one and two pixels, therefore the case where the image is in three pixels is treated in detail in Section II. This process assumes that the image from a point source is circular, that the received optical signal is uniform over the array of pixels, and the pixels are of equal optical responsivity. The method described in this paper has been developed for the case of square pixels, no dead area between pixels, and for uniform photon distribution over the circular image rather than Gaussian or Airy functions. The presented method can be extended to include these characteristics at the cost of considerable complexity especially for the photon distribution function. Practically speaking it is difficult to measure the photon distribution for an optical system and typical measurements are of the nature of 83 percent of the energy in a seeing disc or blur circle of 2 arc-seconds diameter. This amount

of information describing the photon distribution function is appropriate for the presented method.

Since these images fall at random locations on the focal plane, the probability that each image will be in one, two, three, etc., pixels can be calculated based on the geometrical configurations of the image diameters, and pixel sizes. Once these probabilities are known they can be multiplied by the expected maximum signal for one, two, etc. pixels. These partial products can be summed to give the expected maximum signal due to any image as a function of diameter of the image and pixel size. In order to maximize the SNR, the design of most electro-optical systems typically results in the pixel being larger than the expected image diameter and therefore an image rarely falls onto more than four pixels. Due to poor atmospheric "seeing" conditions the image diameter will grow and the occurrence of the image in five or six pixels will increase. The equations required to determine the expected maximum signal and the probabilities when the image is in one to six pixels are given in the next section. Plots (Figs. 5-8) are given that allow the expected signal to be determined without recalculating the equations presented.

The expected maximum signal can then be used in SNR calculations to predict the system performance. This method can also be used to determine what pixel size will give the highest SNR. This is illustrated in section III. Although the electro-optical detection of satellites against a sky background containing stars was the problem that motivated this work, this method is applicable to other detection problems where circular images fall on square pixels.

II. EXPECTED ENERGY DERIVATION

The number of photo-electrons due to a point source, produced by an imaging device at the focal plane of a telescope is:

$$I = p\ a\ q\ t \qquad (1)$$

where: p = photons per second, per unit area, from a point source, at the telescope aperture.

a = product of the telescope aperture area and the telescope optical transmission.

q = imaging device quantum efficiency.

t = integration time.

The calculation of p for solar spectrum point sources, through the earth's atmosphere, can be readily accomplished using reference (2) by R. Weber.

Equation (1) gives the total number of photo-electrons received, but cannot be used directly to calculate the SNR because the calculations depend upon the distribution of energy in x number of pixels. If all the energy is contained in one pixel, the SNR will be higher than if the energy is divided between several pixels.

The definition of SNR is the peak signal divided by the rms noise. The maximum expected energy, as described in Section I, is the peak signal due to an image falling on discrete pixels. The threshold value used for detecting images (or any electrical signal) is determined by measuring the rms noise of the input signal without an image and then selecting a multiple of the rms noise as the threshold value. A detection system can be characterized by measuring its performance vs. the SNR of the input signal. The SNR of the

electro-optical camera is therefore an important parameter. This section describes the maximum energy derivation and Section III demonstrates how this is used to estimate SNR for an electro-optical system.

The distribution of energy from a point source among the imager pixels is dependent upon the size of the circular image, the size of the pixels, and the centroid of the image on the focal plane. Assuming no optical diffraction, the centroids fall randomly on the focal plane, unless the images are maintained in the same locations by tracking. Since it is equally likely that an image centroid will fall on any location within the array, the probabilistic behavior of the system may be derived via geometric analysis.

The well-known expression[3] for the expected value of a discrete random variable

$$E\{s\} = \sum_n S_n P_n, \tag{2}$$

may be interpreted in terms of maximum values. Then,

S_n = the maximum signal possible from a single pixel within the group for n pixels containing all of the signal.

P_n = the associated probability when all of the signal is contained in those n pixels.

$E\{s\}$ = the expected maximum signal.

When all of the I photo-electrons are contained in one pixel, $S_1 = I$; and two pixels, $S_2 = I/2$.

The method used to obtain S_3, S_4, S_5, and S_6 is identical, therefore only calculation of S_3 will be explained in detail. A point source circular image of diameter D can be contained in three square pixels of side L in a finite number of positions. As long as D and L are in the same units all the

following equations are valid. The position of the image can be uniquely specified by the location of the image center, since D and L are known. Figure 1 shows the possible locations of the image center when an image is contained in any three pixel combinations. Since the image center can only be in the four indicated areas, and since these are identical and symmetric, further examinations of only one of these areas is sufficient. Figure 2 shows one of these areas and its relationship to D and L. Therefore the expected location of the image center is the centroid of the area shown in Fig. 2 (point k). Knowing the expected location of the image center and the image, the ratios of area in the three pixels to the total image area can be calculated. These ratios multiplied by I give the expected signal in each of the three pixels. The largest of these ratios is the only one of interest because if it crosses a detection threshold, the point source is detected. If the largest signal among the three pixels doesn't cross the threshold, the other two will not, and there will be no detection.

A. Derivation of S_3

Due to geometric contraints there are only three ranges of D and L that have different expressions for S_3; $D \leq L$, $L < D \leq 1.17L$, and $1.17L < D$. Range $1.17L < D$ results in $S_3 = 0$ because and image of this diameter cannot fit in three pixels. Figure 3 shows the variables used to calculate S_3, x is the distance from the pixel center to the expected location of the image center (point k). A_t is the area of the image and A_2 is the area of the image not in the pixel with the maximum energy. For the range $0 < D \leq L$:

$$S_3 = \frac{A_t - 2A_2}{A_t} I = 0.87\ I \qquad (3)$$

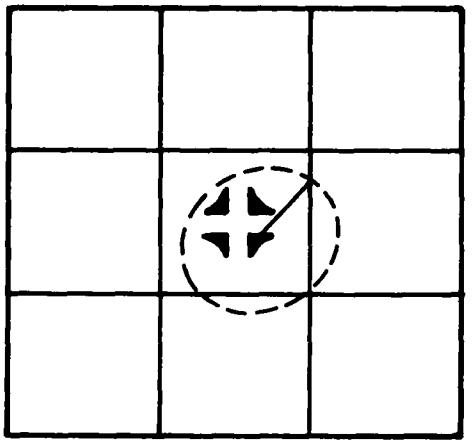

135864-N
135955-N

Fig. 1. Possible locations of image center in three pixels.

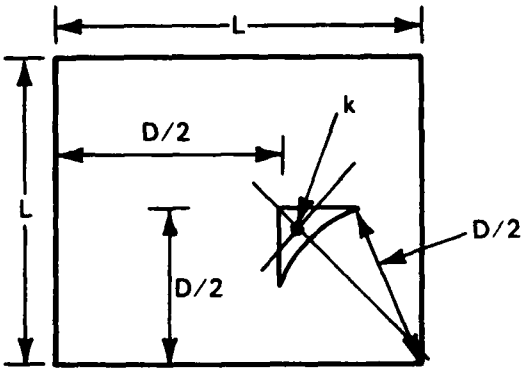

Fig. 2. One of the image center location areas for three pixels.

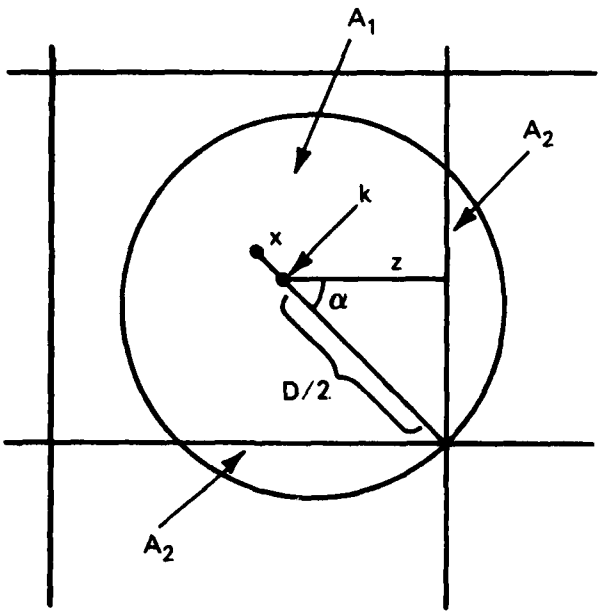

135956-N

Fig. 3. Variables used to determine S_3.

where:

$$A_t = \pi(D/2)^2$$

$$z = 0.38\ D$$

$$A_2 = \frac{\pi D^2}{720} \cos^{-1}\left(\frac{2z}{D}\right) - z\left(\frac{D^2}{4} - z^2\right)^{1/2}$$

A_t is defined the same for all S_n. For the range $L < D \leq 1.17L$:

$$S_3 = \frac{A_t - 2A_2}{A_t} I \tag{4}$$

where: $\alpha = \cos^{-1}\left(\frac{L-D/2}{D/2}\right)$

$$x = \left(1/2\ (L-D/2)^2 - \frac{(45-\alpha)\pi D^2}{1440} - \left(\frac{DL}{4} - \frac{D^2}{8}\right) \sin\alpha\right)^{1/2}$$

$$z = L - D/2 - x \cos 45°$$

The values of S_3 for this range vary from 0.87 I to 0.83 I.

B. Derivation of S_4

There are five ranges of D and L for S_4; $D \leq L$, $L < D \leq 1.17\ L$, $1.17\ L < D \leq 1.25\ L$, $1.25 < D \leq 2L$, and $2L < D$. $S_4 = 0$ for $2L < D$. For the range $D \leq L$:

$$S_4 = .25\ I \tag{5}$$

For the range $L < D \leq 1.17L$:

$$S_4 = \left(.25\ E_1 + \frac{A_{h2}}{A_t} E_2\right) I \tag{6}$$

where: $E_1 = \frac{A_1}{A_1 + A_2}$, $E_2 = \frac{A_2}{A_1 + A_2}$

$$A_1 = \left(\frac{LS}{2} - \frac{S^2}{4}\right) \sin \alpha + \left(\frac{90 - 2\alpha}{1440}\right) \pi D^2$$

$$A_2 = \left(\frac{DL}{2} - \frac{D^2}{4}\right) \cos g + \frac{DL}{4} (6 - \sin w)$$

$$- L^2 - \frac{D^2}{2} - \left(\frac{90 - w - g}{720}\right) \pi D^2$$

$$g = \sin^{-1} \left(\frac{2L - D}{D}\right)$$

$$w = \cos^{-1} (L/D)$$

$$u = \cos^{-1} (.7L/D)$$

$$A_{h2} = A_t - \left(\frac{u + 2w}{720}\right) \pi D^2 + (.35 \sin u + \sin w) \frac{DL}{2}$$

The values of S_4 for this range vary from 0.25 I to 0.30 I. For the range $1.17 L < D \leq 1.25 L$:

$$S_4 = (.25 E_1 + \frac{A_{h2}}{A_t} E_2) I \qquad (7)$$

where: $A_1 = (L - \frac{D}{2})^2$

$$A_2 = L^2 - (1/2 + 1/4 \sin w) DL - \left(\frac{90 - w - \alpha}{720}\right) \pi D^2$$

$$- (L/2 - D/4) D \sin \alpha$$

$$v = \cos^{-1} \frac{.77L}{D}$$

$$A_{h2} = A_t - \left(\frac{v + 2w}{720}\right) \pi D^2 + (.35 \sin v + \sin w) \frac{DL}{2}$$

The values of S_4 for this range vary from 0.25 I to 0.28 I. For the range $1.25\ L < D < 2L$:

$$S_4 = .25\ I \tag{8}$$

C. Derivation of S_5

There are six ranges of D and L for S_5; $D \leq L$, $L < D \leq 1.17\ L$, $1.17\ L < D \leq 1.25$, and $1.25\ L < D \leq 1.41\ L$, $1.41\ L \leq D \leq 2L$ and $2L < D$. $S_5 = 0$ for ranges $D \leq L$ and $2L < D$. For the range $L < D \leq 1.17\ L$:

$$S_5 = \left(\frac{A_{h1}}{A_t}\ E_1 + \frac{A_{h2}}{A_t}\ E_2\right) I \tag{9}$$

where:
$$A_{h1} = \frac{\sin^{-1}(L/D)}{720}\ D^2\pi + .75L\ (D^2 - L^2)^{1/2}$$

$$A_{h2} = A_t - \frac{w}{180}\ \pi\ D^2 + L\ (D^2 - L^2)^{1/2}$$

$$A_1 = \left(\frac{90 - g - 2w}{720}\right) \pi\ D^2 + \frac{DL}{2} \sin w - \left(\frac{DL}{2} - \frac{D^2}{4}\right) \cos g$$

$$A_2 = \left(\frac{D}{2} - \frac{L}{2}\right)^2$$

The values of S_5 for this range vary from 0.57 I to 0.78 I. For the range $1.17\ L < D \leq 1.25\ L$:

$$S_5 = \left(\frac{A_{h1}}{A_t}\ E_1 + \frac{A_{h2}}{A_t}\ E_2\right)\ I \tag{10}$$

where: $A_1 = \frac{LD}{2} \sin w + \left(\frac{D}{2} \sin \alpha - L + \frac{D}{2}\right)^2 / \tan \alpha$

$$+ \left(\frac{90 - \alpha - 2w}{720}\right) \pi D^2 - \left(L - \frac{D}{2}\right)^2 \tan (90 - \alpha)$$

$$A_2 = \left(\frac{D - L}{2}\right)^2 - \left(\frac{\alpha - 45}{720}\right) \pi D^2 + 1.41 \left(\frac{DL}{2} - \frac{D^2}{4}\right) \sin (\alpha - 45)$$

The values of S_5 for this range vary from 0.76 I to 0.78 I. For the range $1.25\ L < D \leq 1.41\ L$

$$S_5 = \left(\frac{A_{h1}}{A_t} E_1 + \frac{A_{h2}}{A_t} E_2\right) \quad I \tag{11}$$

where: $A_1 = DL - \frac{D^2}{2} - (L - \frac{D}{2}) (LD - L^2)^{1/2} + \left(\frac{w + \alpha - 135}{720}\right) \pi D^2$

$$A_2 = \frac{L^2}{4} - \frac{DL}{4} \sin w - \left(\frac{90 - 2w}{1440}\right) \pi D^2$$

The values of S_5 for this range vary from 0.73 I to 0.80 I. For the range $1.41\ L < D \leq 2L$:

$$S_5 = \left(\frac{A_{h1}}{A_t} E_1\right) \quad I \tag{12}$$

where: $A_1 = DL - \frac{D^2}{2} - (L - \frac{D}{2}) (DL - L^2)^{1/2}$

$$- \left(\frac{180 - 2\alpha}{1440}\right) \pi D^2$$

The values of S_5 for this range vary from 0.58 I to 0.73 I.

D. Derivation of S_6

There are five ranges of D and L for S_6; $D \leq L$, $L < D \leq 1.17\ L$, $1.17\ L < D \leq 1.25\ L$, $1.25\ L < D \leq 2L$, $2L < D$. $S_6 = 0$ for ranges $D \leq L$ and $2L < D$.

For the range $L < D \leq 1.17\ L$:

$$S_6 = \left(\frac{A_h}{A_t}\right) I \tag{13}$$

where: $A_h = \left(\frac{90 - w}{720}\right) D^2\Pi + \frac{L}{4}(D^2 - L^2)^{1/2}$

The values of S_6 for this range vary from 0.47 I to 0.50 I.

For the range $1.17\ L < D \leq 1.25\ L$:

$$S_6 = \left(\frac{A_{h1}}{A_t} E_1 + \frac{A_{h2}}{A_t} E_2\right) I \tag{14}$$

where: $A_{h1} = \left(\frac{90 - w}{720}\right) D^2\Pi + \frac{L}{4}(D^2 - L^2)^{1/2}$

$$A_{h2} = \left(\frac{135 - \alpha}{720}\right) D^2\Pi + (L - \tfrac{D}{2})^2 + \left(\frac{LD}{2} - \frac{D^2}{4}\right) \sin\alpha$$

$$A_1 = \frac{j}{720} D^2\Pi - \frac{L}{4}(D^2 - L^2)^{1/2}$$

$$A_2 = \left(\left(\frac{90 - 2g}{360}\right) D^2\Pi - 2.82\,(LD - \frac{D^2}{2}) \sin(45 - g)\right) / 4L^2$$

$$j = \tan^{-1}\left((D^2 - L^2)^{1/2}/L\right)$$

The values of S_6 for this range vary from 0.45 I to 0.47 I.

For the range $1.25\ L < D \leq 2L$:

$$S_6 = \left(\frac{A_h}{A_t}\right) I \tag{15}$$

where: $A_h = (L - \frac{D}{2})^2 + \left(\frac{DL}{2} - \frac{D^2}{4}\right) \sin\alpha + \left(\frac{135 - \alpha}{180}\right) A_t$

The values of S_6 for this range vary from 0.28 I to 0.45 I.

The method used to derive the expressions for P_n is similar to that used to obtain expressions for S_n. When an image center falls at random on the focal plane the P_n is equal to the area that the center can occupy while the image is contained in exactly n pixels, divided by the area of one pixel. Figure 1 shows this area for n = 3. The expressions for P_n are a function of D and L, and change for various ranges of D and L.

$$P_1 = (L - D)^2/L^2 \qquad D < L \tag{16}$$

$$P_1 = 0 \qquad L \leq D$$

$$P_2 = 2D\ (L - D)/L^2 \qquad D < L \tag{17}$$

$$P_2 = 0 \qquad L \leq D$$

$$P_3 = D^2\ (1 - \Pi/4)/L^2 \qquad D < L \tag{18}$$

$$P_3 = \left(D^2\ (1 + \sin\alpha - \Pi\left(\frac{45-\alpha}{180}\right)\right) - DL\ (4 + 2\sin\alpha) + 4L^2\Big)/L^2 \qquad L \leq D < 1.17\ L \tag{19}$$

$$P_3 = 0 \qquad 1.17\ L \leq D$$

$$P_4 = D^2\Pi/4L^2 \qquad D < L$$

$$P_4 = \Big(DL\ (6 + 2\cos g + 2\sin\alpha - \sin 2e) - 4L^2 - D^2\ (2 + \cos g + \sin\alpha + \frac{\Pi}{180}\ (45 - 2e - g + \alpha)\Big)/L^2 \qquad L \leq D < 1.17\ L \tag{20}$$

where: $g = \sin^{-1}\ \left((2L - D)/D\right)$

$$P_4 = \Big(D^2\ (1 + \sin\alpha - \frac{\Pi}{180}\ (90 - 2e - \alpha) - DL\ (6 + \sin 2e + 2\sin\alpha) + 8L^2\Big)/L^2 \qquad 1.17\ L \leq D < 1.25\ L \tag{21}$$

$$P_4 = (4L^2 - 4DL + D^2)/L^2 \qquad 1.25\ L \leq D < 2L \tag{22}$$

$$P_4 = 0 \qquad 2L \leq D$$

$$P_5 = 0 \qquad D < L$$

$$P_5 = \Big(D^2\ (1 + \Pi/180\ (90 - \alpha - 4e) + \cos\alpha) + DL\ (2 \sin 2e - 2 - 2\cos\alpha) + L^2\Big)/L^2 \tag{23}$$

$$L \leq D < 1.17\ L$$

$$P_5 = \Big(D^2\ (1 + \Pi/90\ (67.5 - \alpha - 2e) - 1.41 \sin(\alpha - 45)\Big) + DL\Big(2 \sin(2e) - 2 + 2.83 \sin(\alpha - 45)\Big) + L^2 - (2L - D)^2 \tan(90 - \alpha) + (D \sin\alpha - 2L + D)^2/\tan\alpha\Big)/L^2 \tag{24}$$

$$1.17\ L \leq D < 1.25\ L$$

$$P_5 = \Big(DL\ (4 - \sin(2e)) + D^2\ (\Pi/180\ (2e + \alpha - 135) - 2) + L^2 - (4L - 2D)\ (DL - L^2)^{1/2}\Big)\ L^2 \tag{25}$$

$$1.25\ L \leq D < 1.41\ L$$

$$P_5 = \Big(4DL - D^2\ (2 + \Pi/360\ (180 - 2\alpha)) - (4L - 2D)\ (DL - L^2)^{1/2}\Big)/L^2 \tag{26}$$

$$1.41\ L \leq D < 2L$$

$$P_5 = 0 \qquad 2L < D$$

$$P_6 = 0 \qquad D < L$$

$$P_6 = \Big(\tan^{-1}\ (2\ (D^2/4 - L^2/4)^{1/2}/L)\ \Pi\ D^2/180 - 2L\ (D^2/4 - L^2/4)^{1/2}\Big)/L^2 \tag{27}$$

$$L \leq D < 1.17\ L$$

$$P_6 = \Big(D^2\ \Pi/360\ (90 - 2g + 2\tan^{-1}\ (2\ (D^2/4 - L^2/4)^{1/2}/L)) - 2L\ (D^2/4 - L^2/4)^{1/2} - 2.83\ (DL - D^2/2) \sin(45 - g)\Big)/L^2 \tag{28}$$

$$1.17\ L \leq D < 1.25\ L$$

$$P_6 = \Big((D - L/\cos g)^2 \sin g \cos g - L^2 (4 + \tan g) + DL (2 \cos g + 2 \sin 2e) + D^2 (1 + \pi/180) (45 - 2g - 4e - \cos g)\Big)/L^2 \qquad (29)$$

$$1.25\ L \leq D < 2L$$

$$P_6 = 0 \qquad 2L < D$$

The equations for P_n where n = 1 to 6 can be used to calculate the probability of an image of diameter D being in 1 to 6 pixels of side L for any combination of D and L. Figure 4 is a plot of P_n where L = 4 and D varies from 0 to 8. An image D = 3 falling on a focal plane with pixels of side L = 4 has the probability of being in one pixel P_1 = 0.06, two pixels P_2 =0.38, P_3 = 0.12, P_4 = 0.44, P_5 = 0, and P_6 = 0. The sum of the probabilities is also plotted in Fig. 4 for D = 0 to 1.25 L. At this bound the probability of the image being in seven pixels begins to be greater than zero, and at 1.41 L the probability of being in eight pixels begins to be greater than zero.

Review of equations (3) through (15) shows that S_n can be rewritten as:

$$S_n = k_n I \qquad (30)$$

This allows equation (2) to be rewritten:

$$E\{s\} = \sum_n k_n I P_n = I \sum_n k_n P_n \qquad (31)$$

From equation (31) a <u>normalized</u> expected maximum signal can be expressed which shows the dependence on D and L, and independence on I.

$$NOR\ E\{s\} = E\{s\}/I = \sum_n k_n P_n \qquad (32)$$

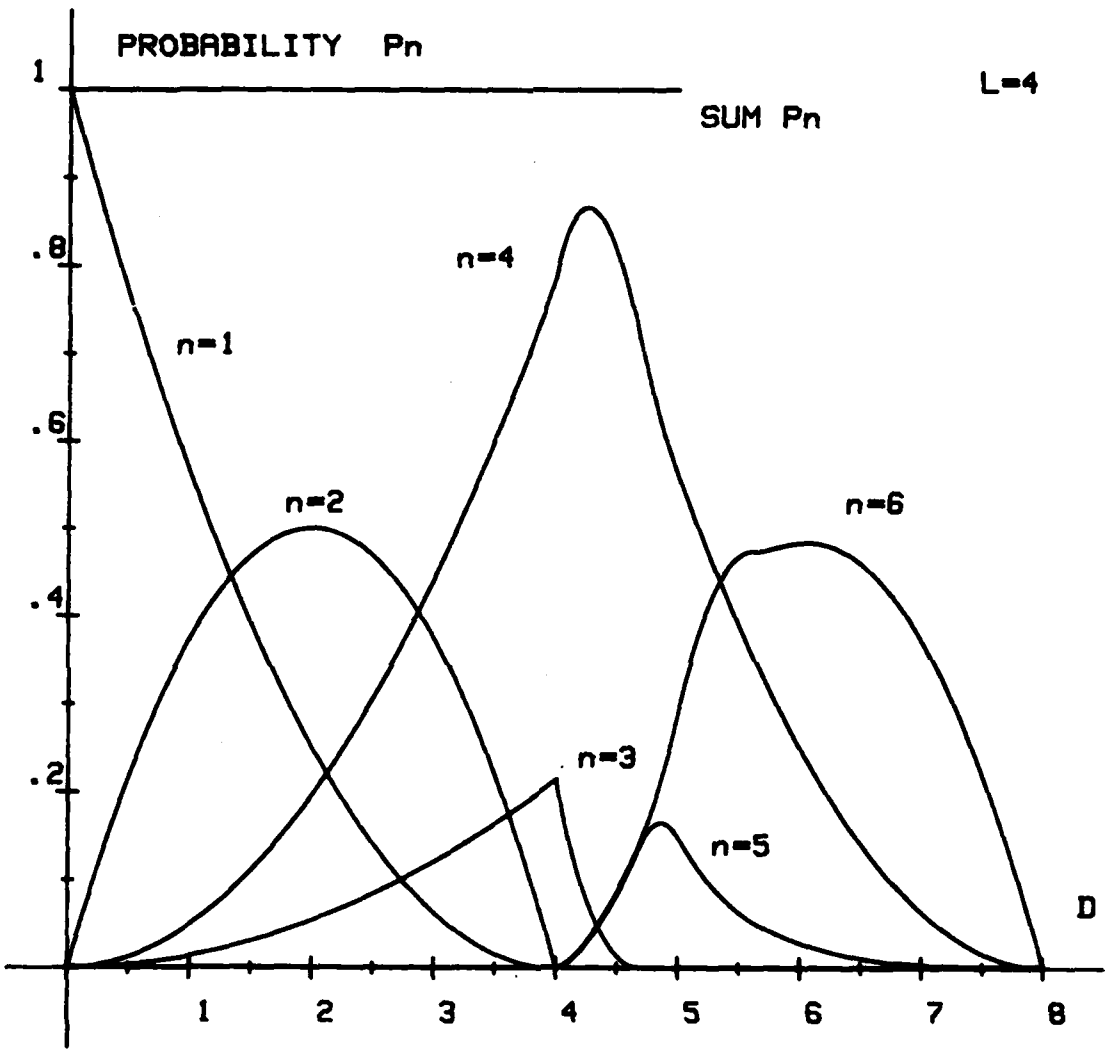

Fig. 4. Probability of an image falling into n pixels for image diameters (D) 0 to 8 and for pixel size L=4.

The values of equation (32) can be viewed as attenuation factors of I that result in the expected signal E{s}. Equation (32) is plotted in Fig. 5 to 8 for many values of D while L varies from D/1.25 to 15. The lower limit of L is again due to the image not being considered in more than six pixels. The values of NOR E{s} increase as L increases which by itself suggests that big pixels give more signal. However while E{s} is the numerator of the SNR, the denominator increases at a much faster rate and results in the important SNR decreasing with large pixel size. This is discussed in the next section.

The relative increase in NOR E{s} when L < D is due to P_5, P_6, S_5 and S_6 increasing. Although P_5 and P_6 would be expected to increase as D becomes larger than L it is not intuitive that S_5 and S_6 should increase. They increase due to the geometric contraints imposed when a circular energy distribution is in 5 or 6 square pixels. This causes the "tails" on the curves in Figs. 5 to 8. Values of S_5 range from 0.73 I to 0.80 I and S_6 from 0.45 I to 0.50 I. Intuitively several people have suggested that S_5 should be 1/5 I and S_6 should be 1/6 I. A simple graphical check will show that this is not possible.

Using the values of NOR E{s} plotted in Figs. 5 to 8, the E{s} may be calculated for any I without having to calculate equations 3 through 29 for a particular combination of D and L. D and L must be in the same units.

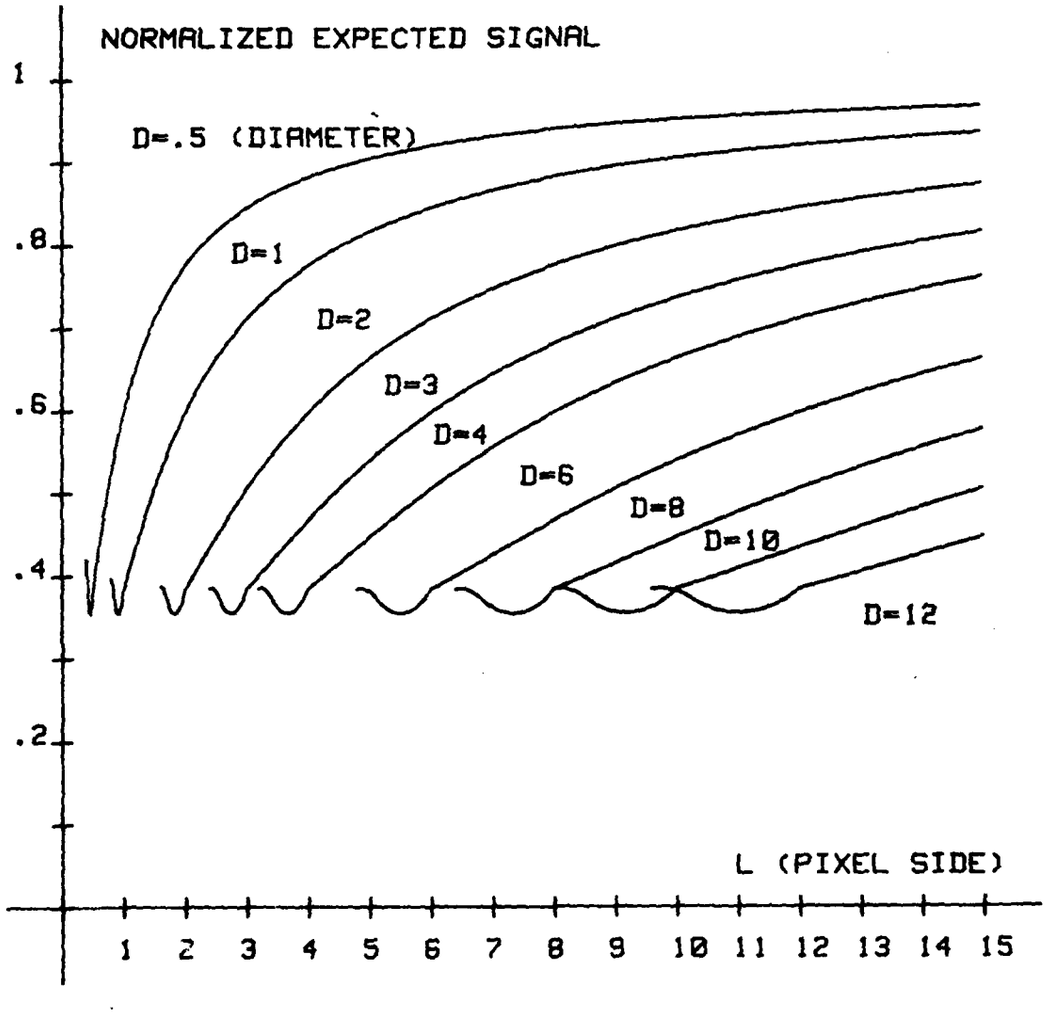

136966-S

Fig. 5. NOR E{s} vs. L for D = .5 to 12.

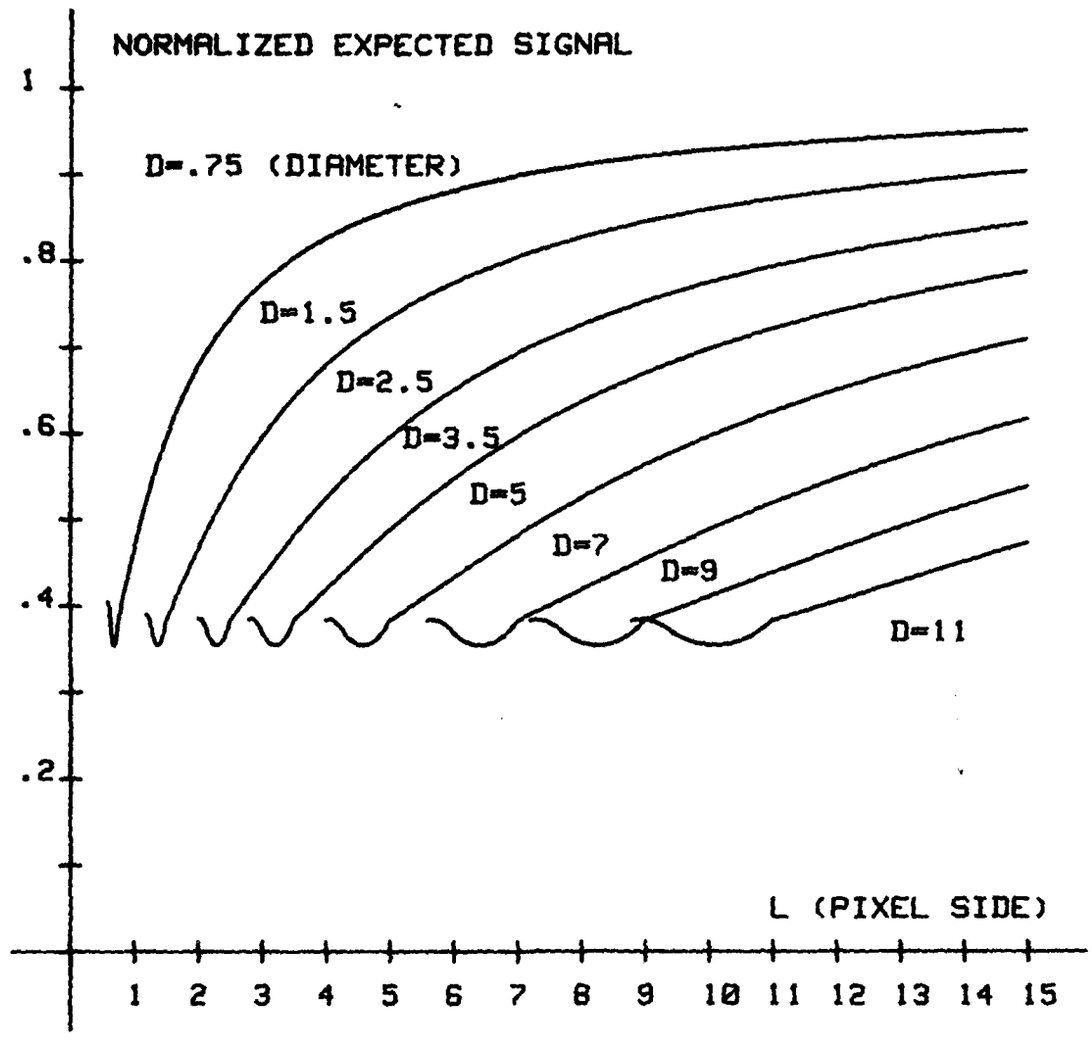

135969-S

Fig. 6. NOR E{s} vs. L for D = .75 to 11.

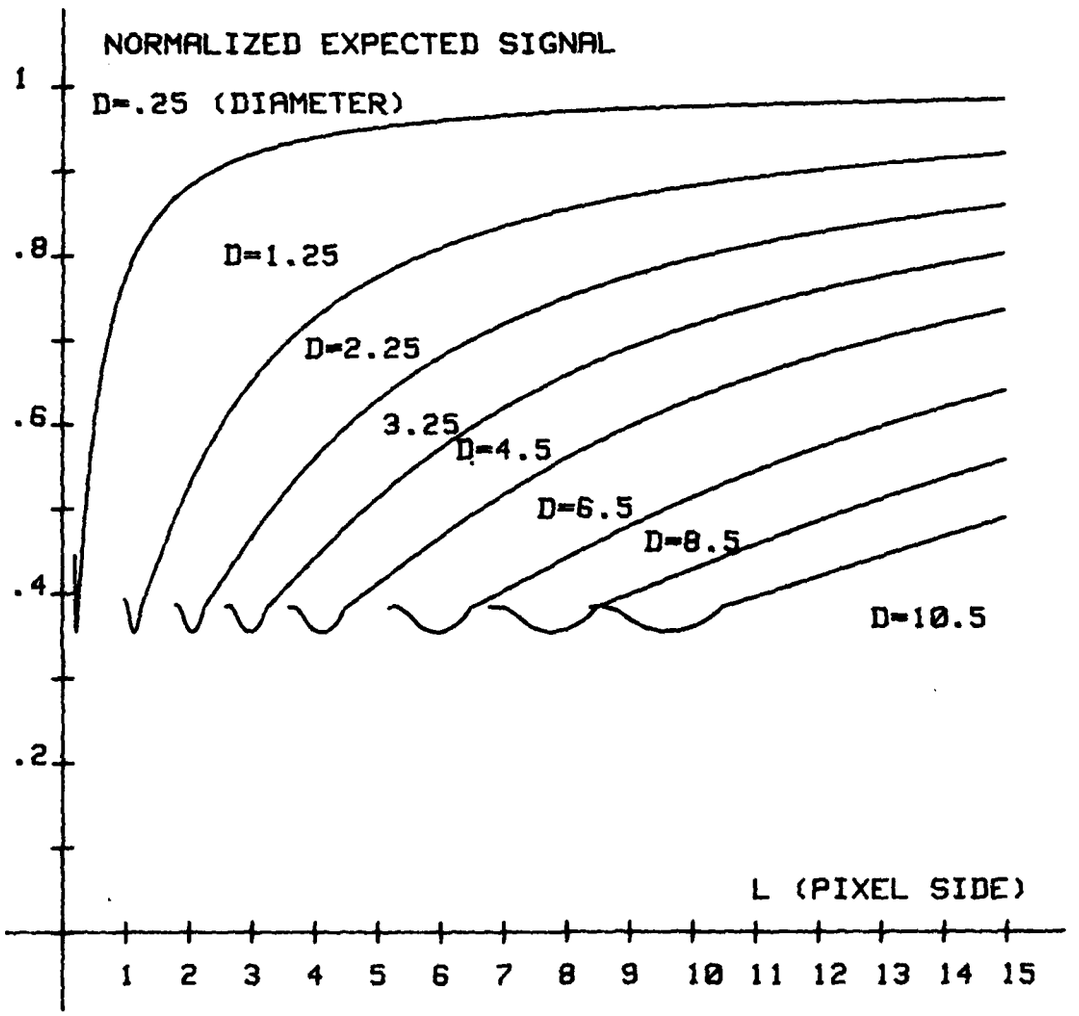

Fig. 7. NOR E{s} vs. L for D = 1.25 to 10.5.

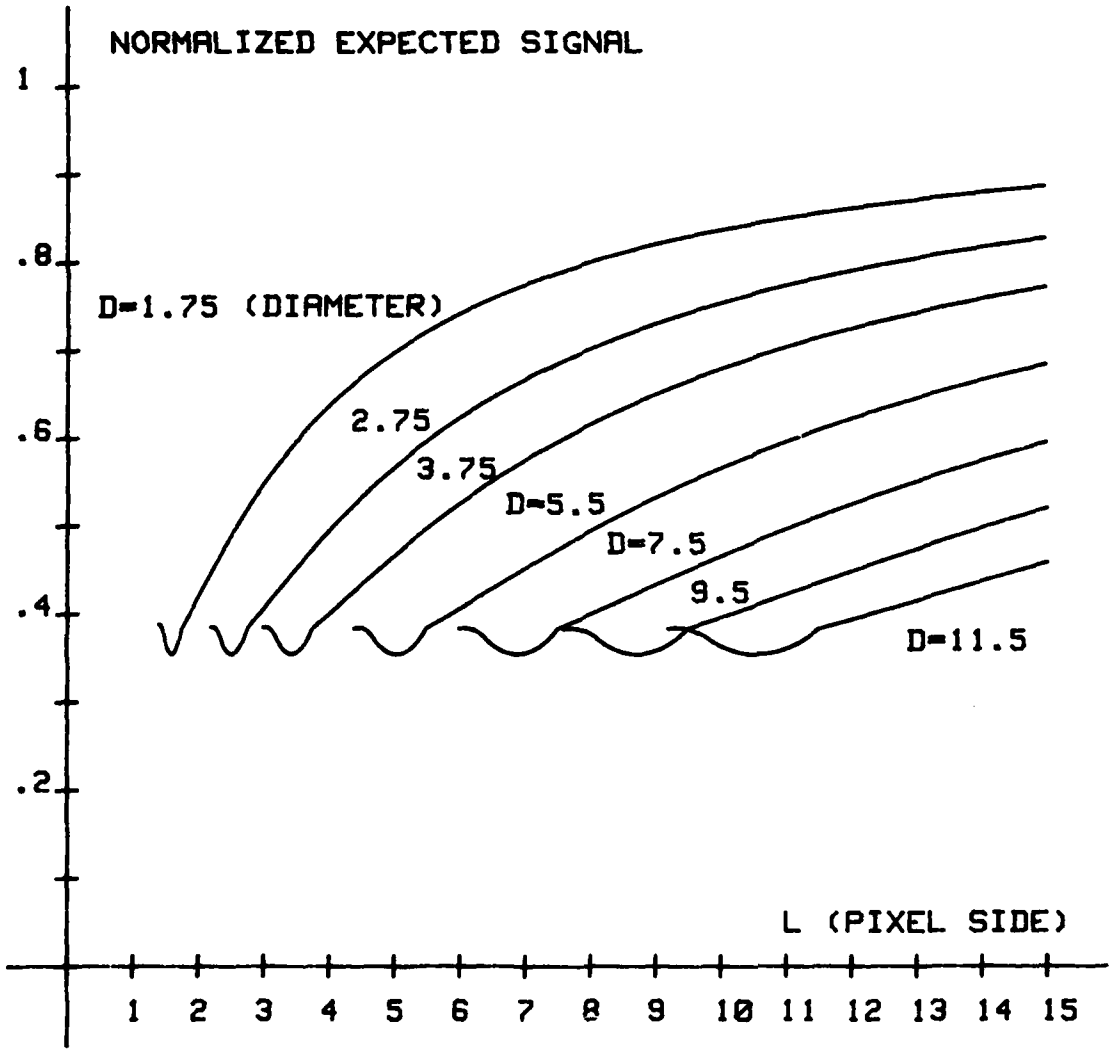

135961-S

Fig. 8. NOR E{s} vs. L for D = 1.75 to 11.5.

III. USING THE EXPECTED ENERGY

The maximum expected energy from a point source can now be determined, and used to calculate SNR.

$$SNR = \frac{E\{s\}}{(B + N^2)^{1/2}} \tag{33}$$

where: B = mean photo-electrons due to background

N = RMS noise electrons of imaging device

The calculation of B is similar to that of I.

$$B = b\ a\ q\ t\ L^2 \tag{34}$$

where: b = photons per second, per unit area, per angular area of sky at the telescope aperture.

The calculation of b can be accomplished using reference (2). The numerator of equation 33 increases as L increases, as shown in Section II using the normalized expected signal. The denominator of equation 33 also increases with L and to demonstrate this increase and dependence of L the denominator divided by $(b\ a\ q\ t + N^2)^{1/2}$ is plotted in Fig. 9 for b = 792, a = 0.46, q = 0.4, t = .6, and N = 20. This results in a normalized plot of the SNR denominator, although not normalized to one.

The input SNR required to produce a specified performance of detection (probability of detection and false alarm rate) is a useful way in which to evaluate the performance of an electro-optical system. In essence, the system is viewed as a "black box". The performance of a detection system as a "black box" can be measured as a function of the input SNR. In many situations, a minimum acceptable SNR is from 6 to 8.[4] An automatic detection system[5]

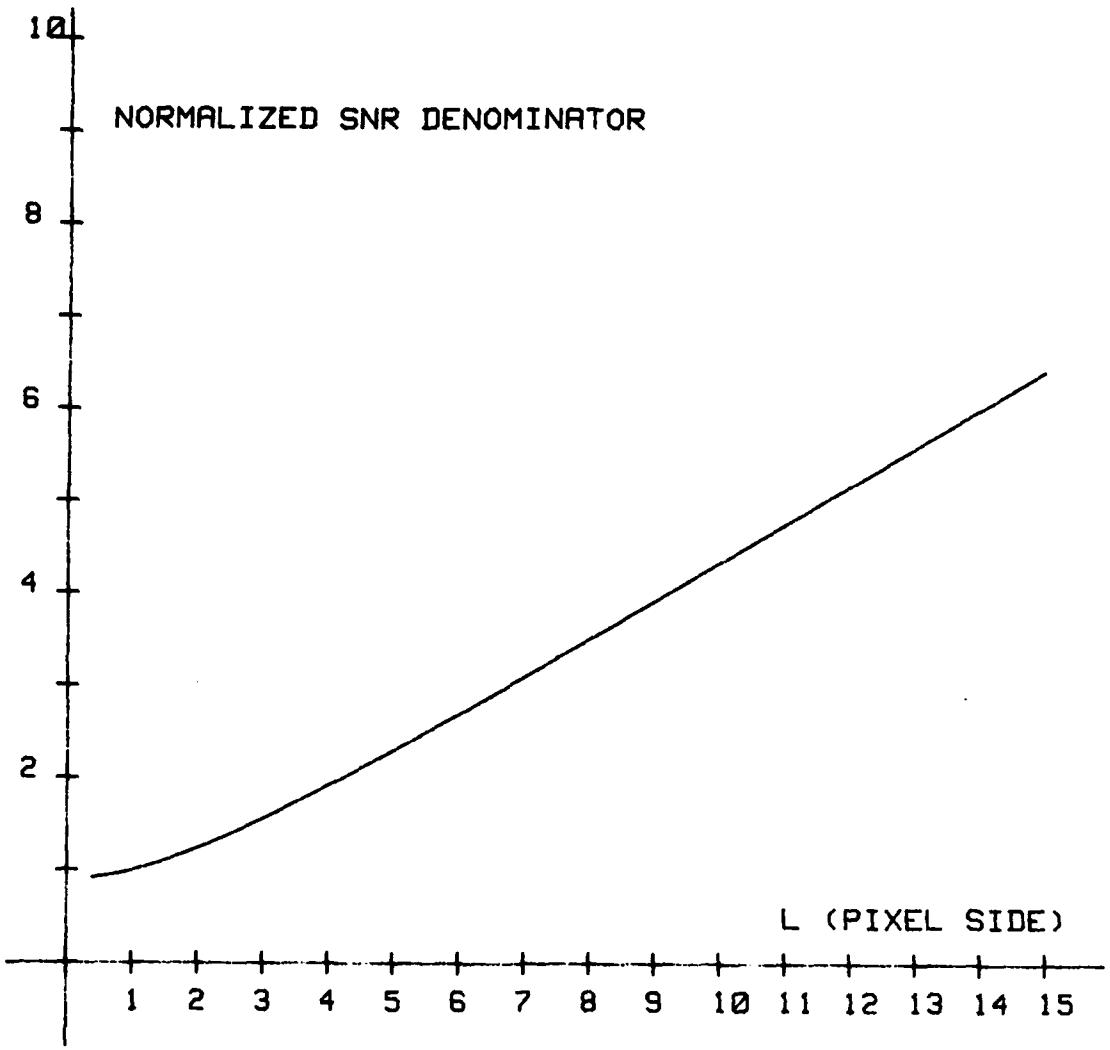

Fig. 9. Normalized SNR denominator dependence on L.

can detect targets with a probability of detection of .95, a false alarm rate of $4.8 * 10^{-3}$, when the SNR is as low as 3.

Plotting SNR using equations (1) through (34) shows the dependence of SNR on L for several values of D. Figures 10 through 18 are plotted with typical parameter values which are listed on each plot. Area is in meters squared, time is in seconds, D and L are in arc-seconds and all other units are specified for equations (1) and (34). All plots start at L = D/1.25 where the image is in six pixels or less. The tails on the plots when L < D is again due to the geometric contraints imposed when a circular image is in 5 or 6 pixels as discussed in Section II.

Figures 10 through 14 are plotted with p (photons from a point source) and b (photons from the background) changing, while the parameters a, q, t, and N are fixed. This is the case in an operating electro-optical system where the satellite and sky are changing in intensity over time. Figures 15 through 18 have all parameters fixed to match Fig. 10 except for one parameter in each figure; i.e., a in Fig. 15, q in Fig. 16, t in Fig. 17, and N in Fig. 18. This demonstrates the degree that the electro-optical system designer can affect SNR.

Although the shape of the SNR plots in Figs. 10 through 18 change, dependent on the parameter values used, it is clear the there is an optimal pixel size to maximize SNR. The importance of pixel size is frequently overlooked while the other controlable parameters a, q, and t, are maximized and N minimized. There is an intuitive feeling that the pixel size should be large in the hope that a point source image will fall in one pixel and therefore give a large signal. While at the same time it is clear that a large pixel will

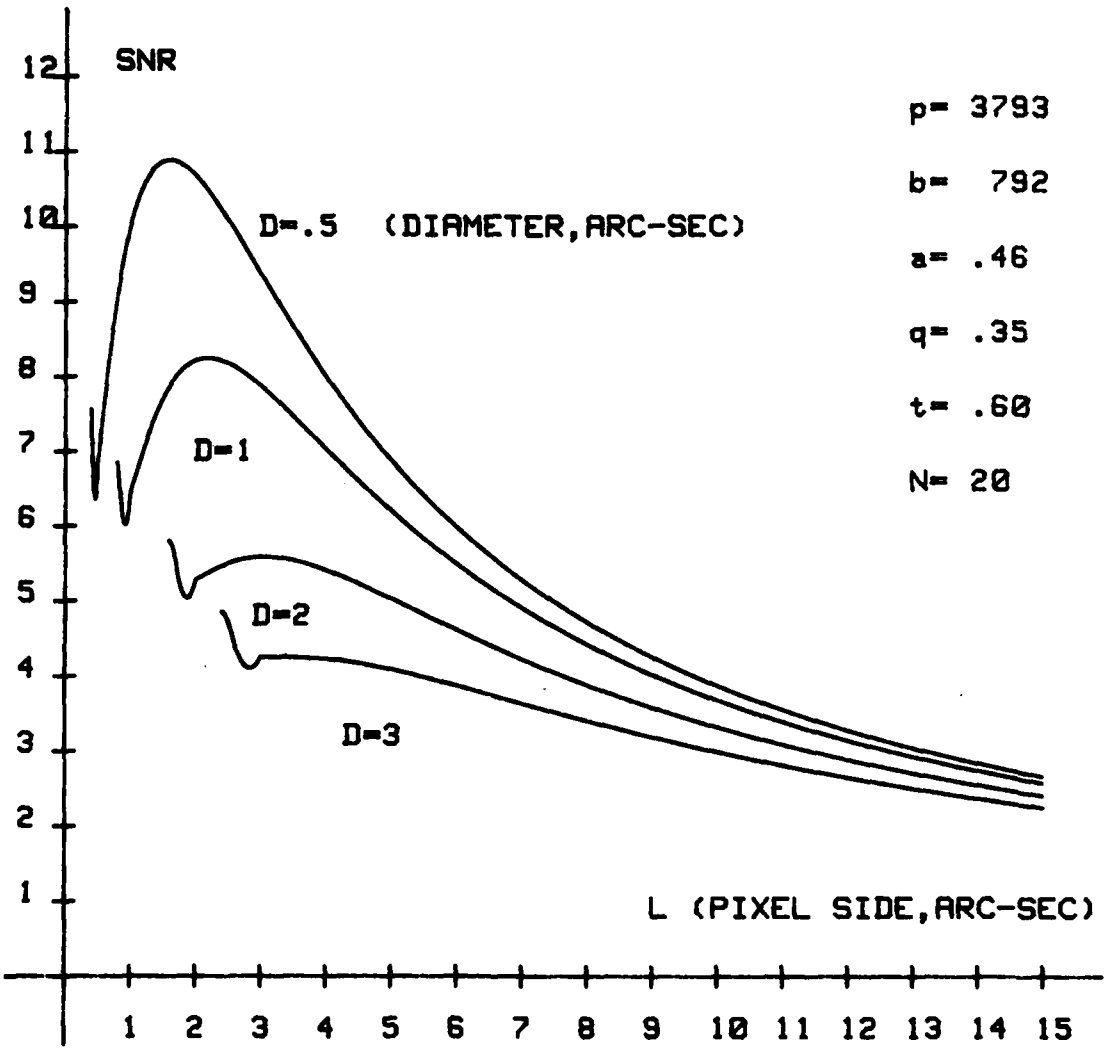

136963-S

Fig. 10. SNR vs. L.

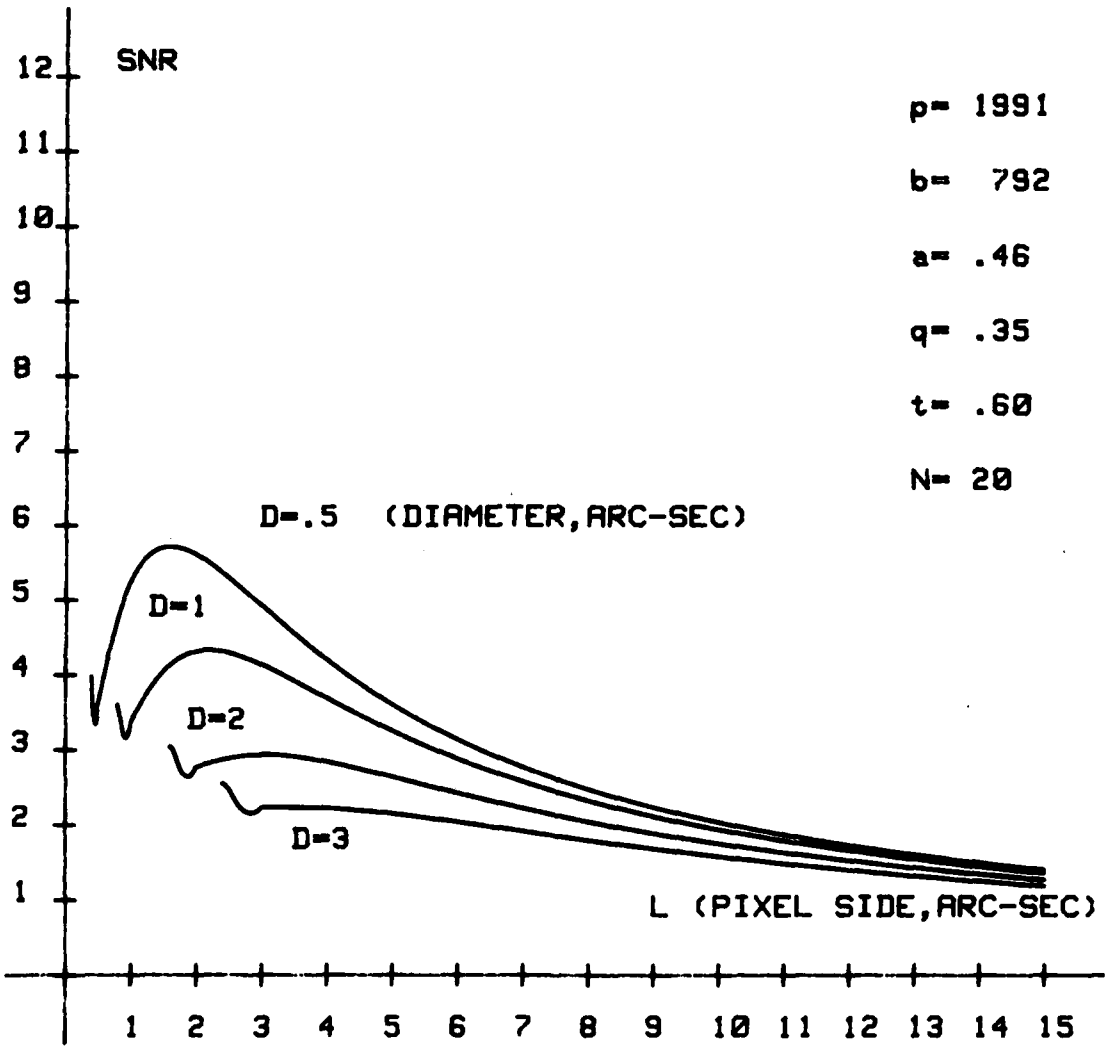

Fig. 11. SNR vs. L, p = 1991.

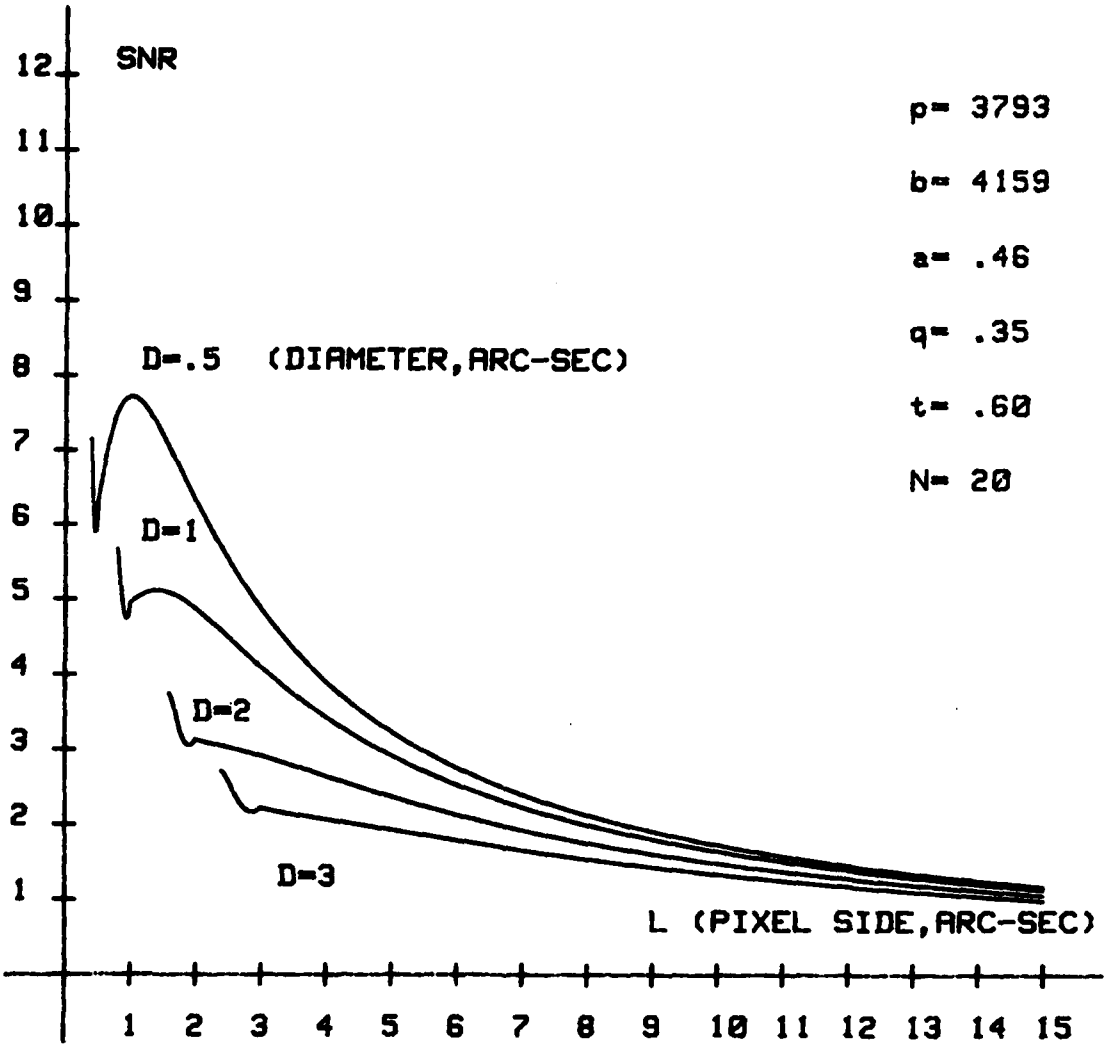

136966-S

Fig. 12. SNR vs. L, b = 4159.

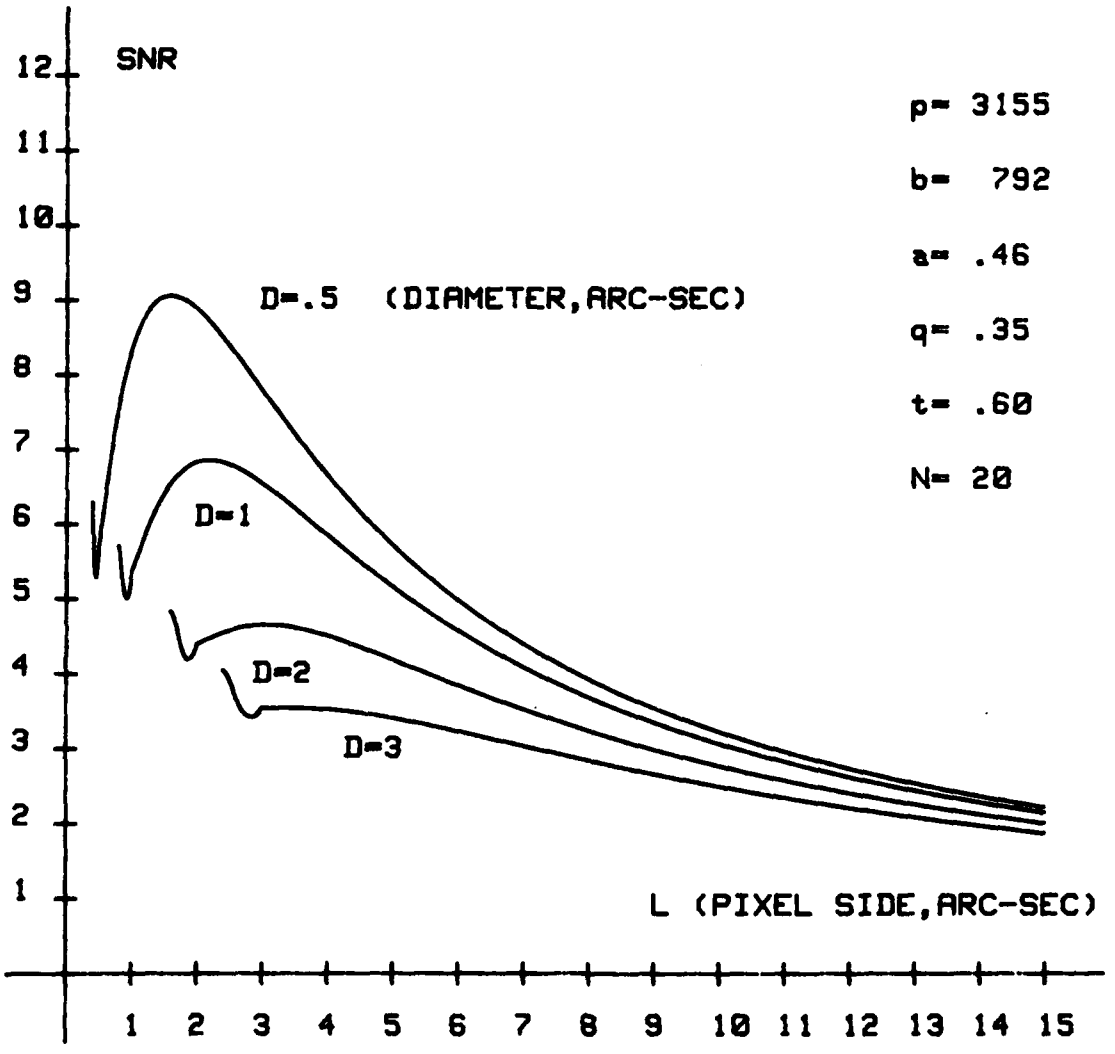

Fig. 13. SNR vs. L, p = 3155.

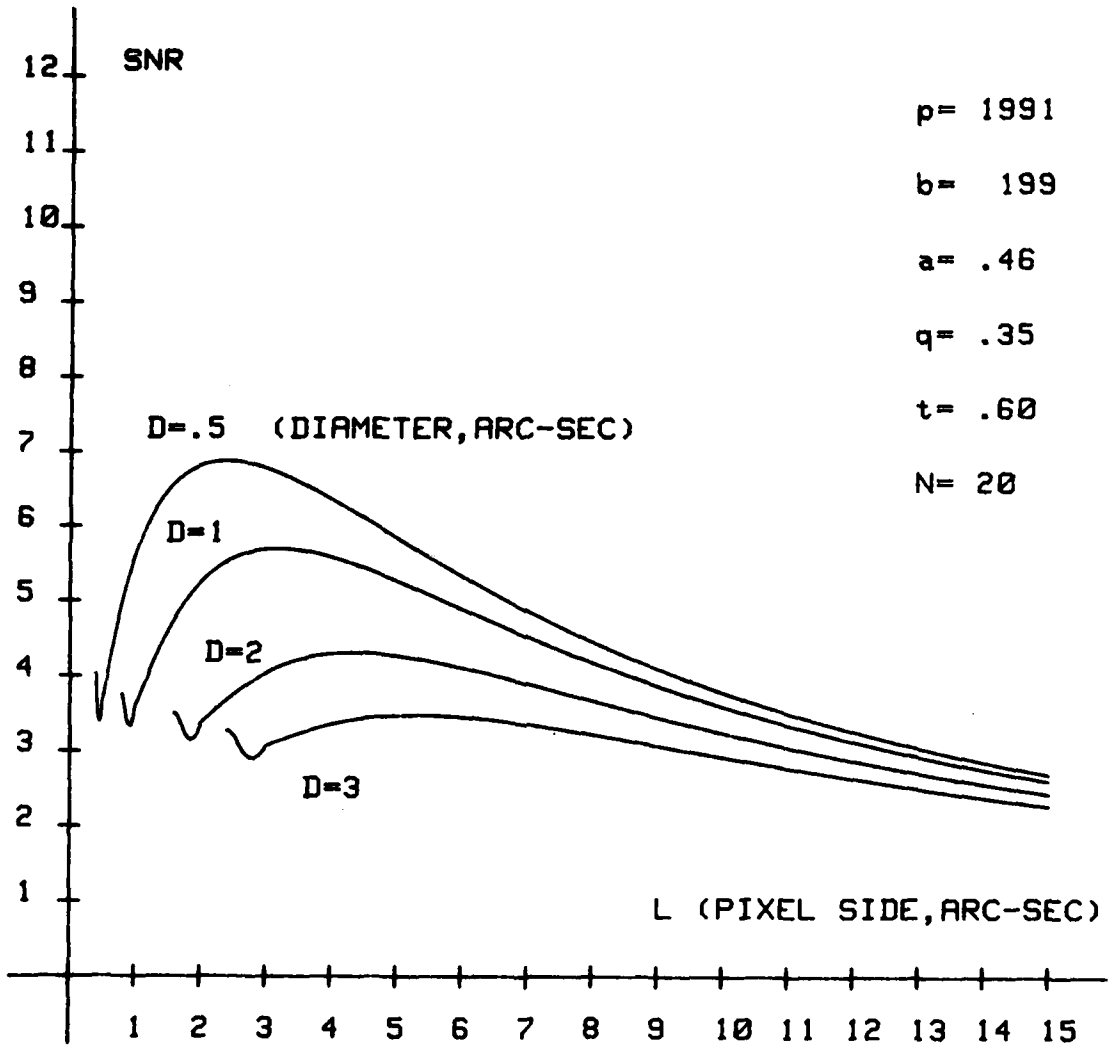

Fig. 14. SNR vs. L, p = 1991, b = 199.

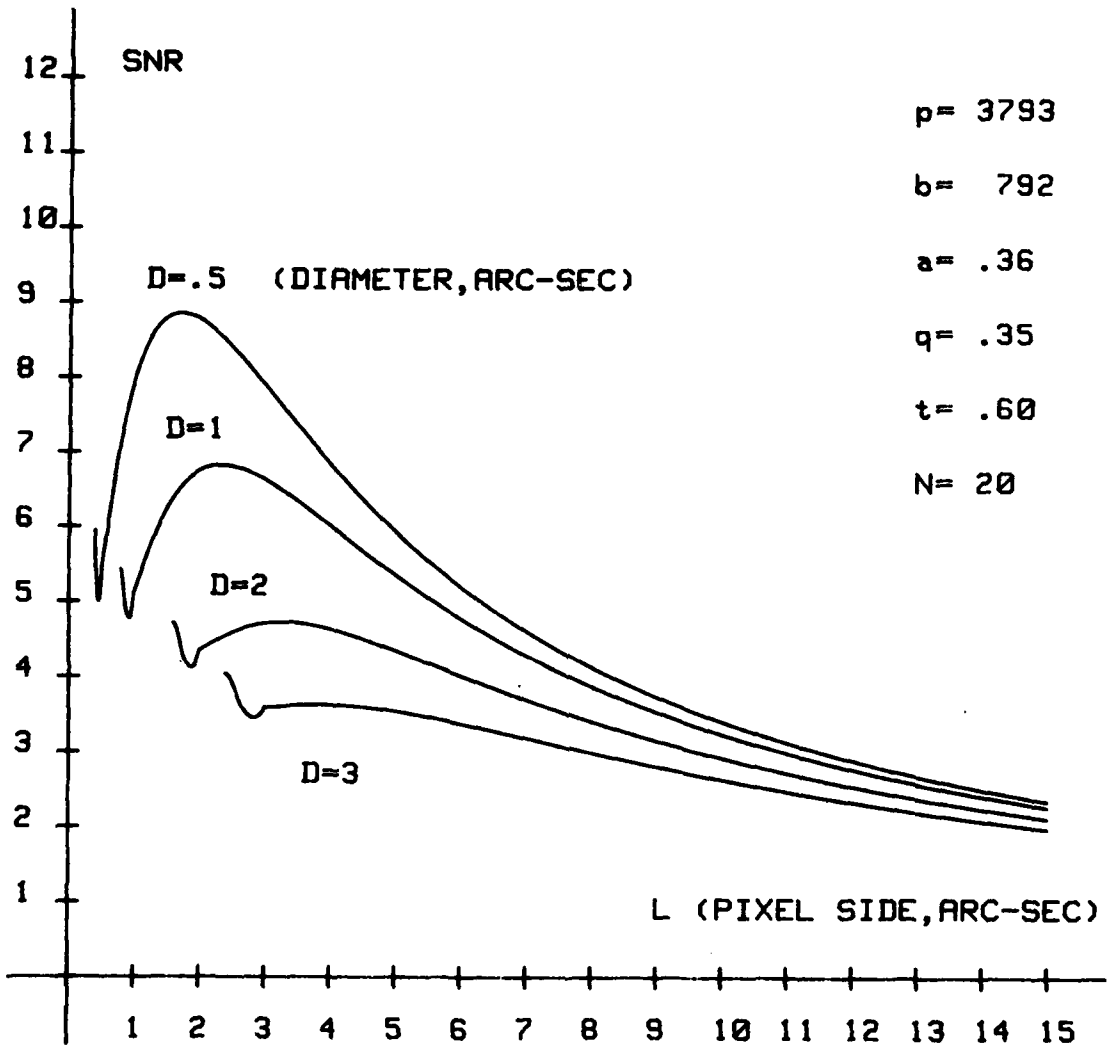

Fig. 15. SNR vs. L, a = .36.

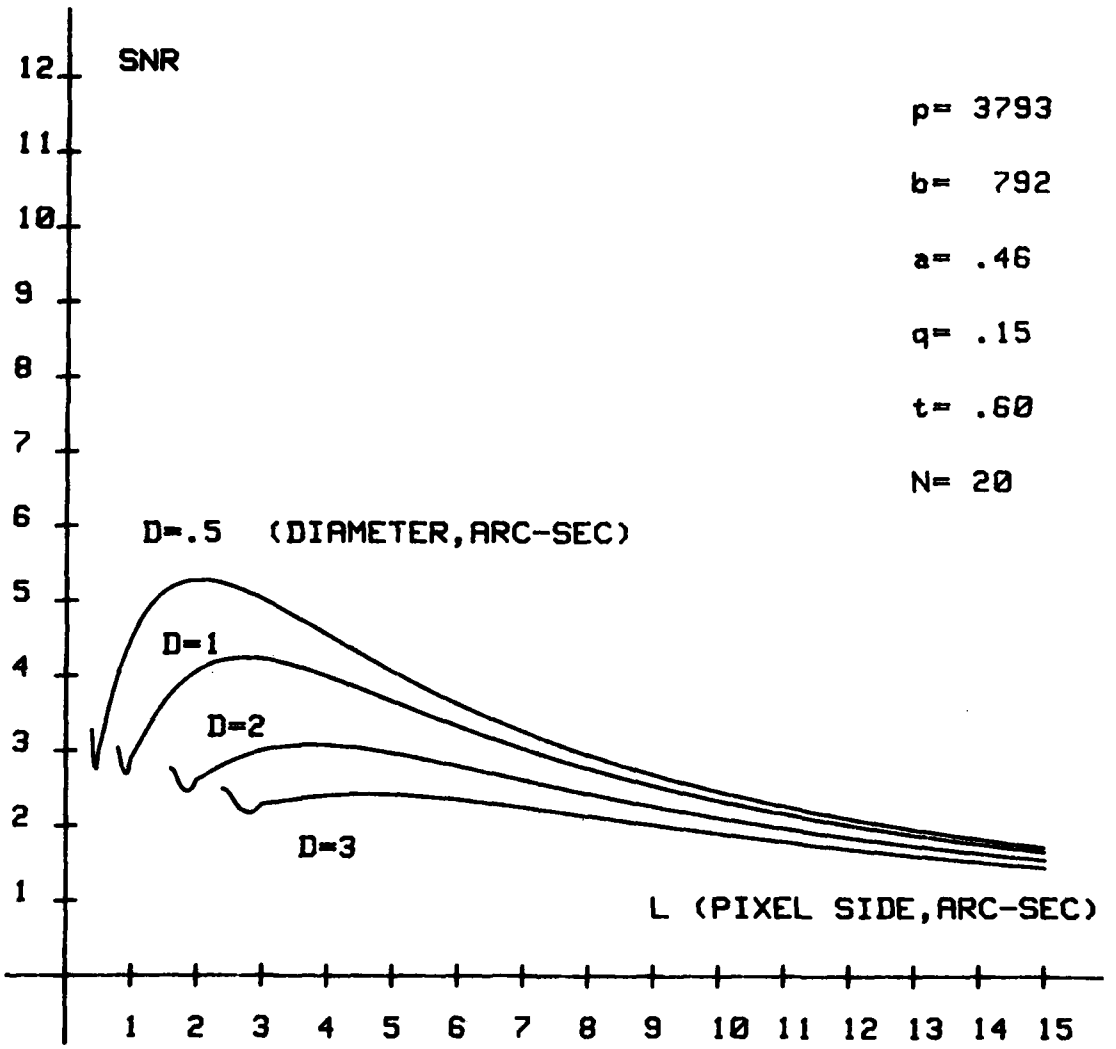

135969-S

Fig. 16. SNR vs. L, q = .15.

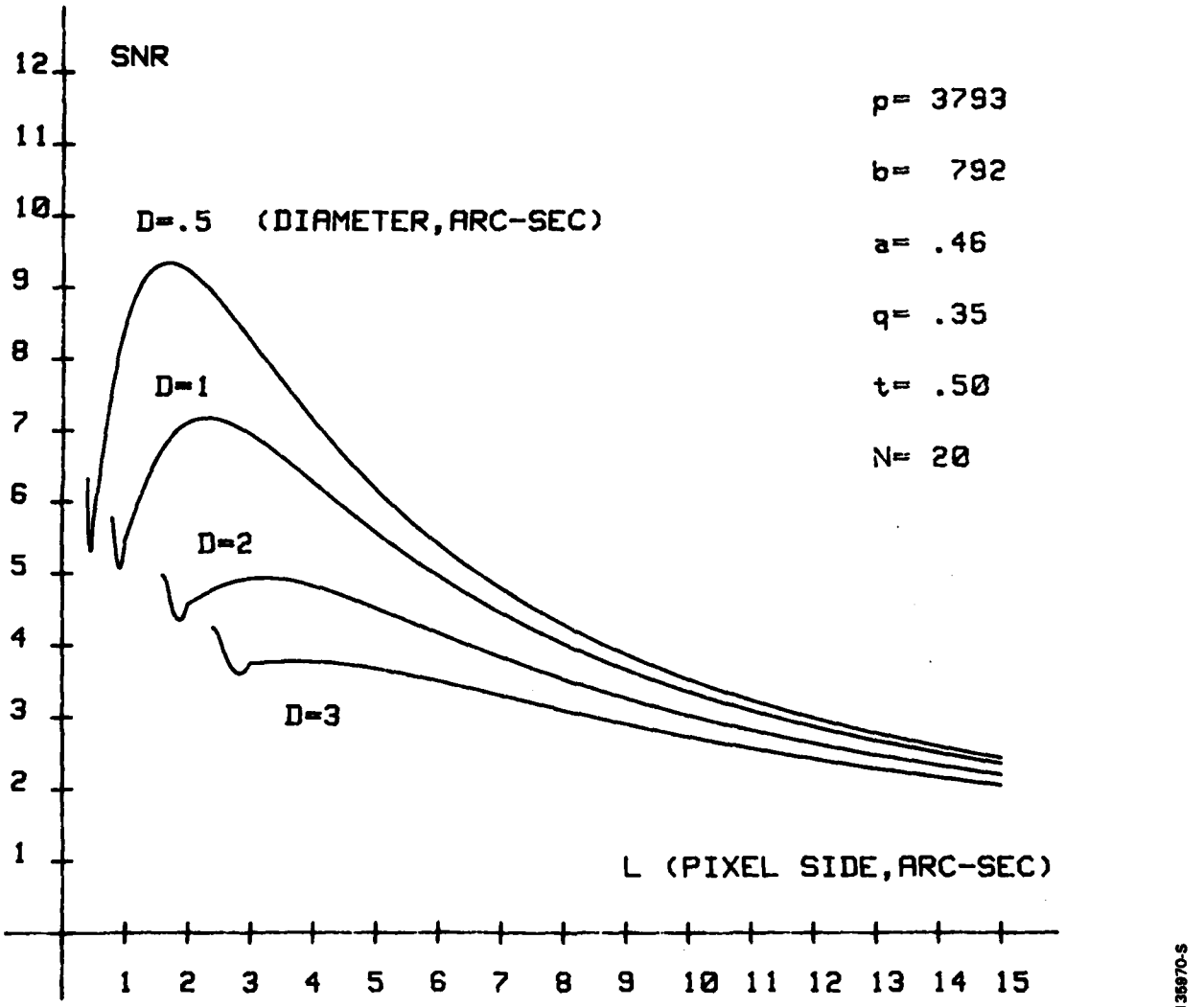

Fig. 17. SNR vs. L, t = .50.

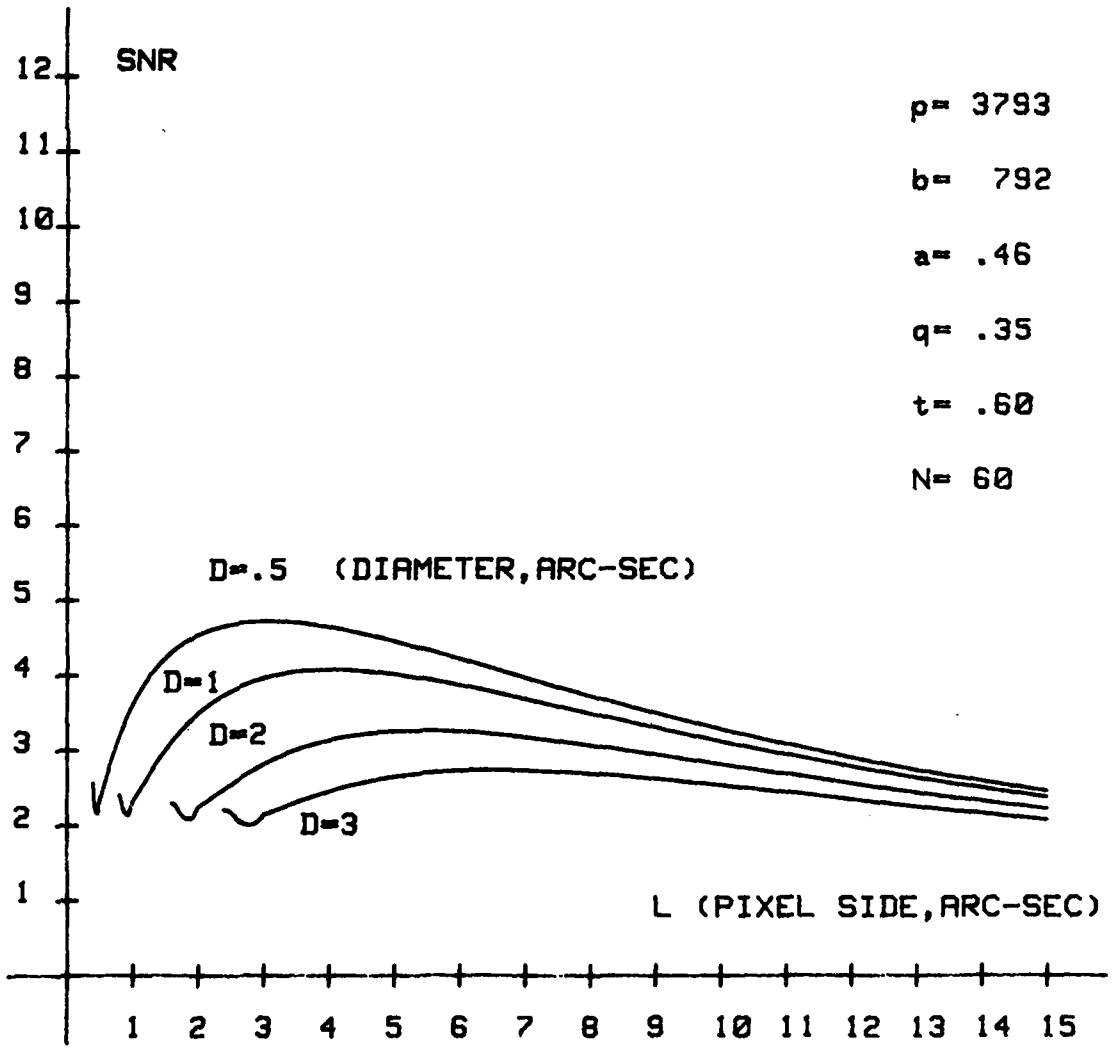

135971-S

Fig. 18. SNR vs. L, N = 60.

collect more background photons which will increase the noise. The method of estimating the expected maximum signal derived in this paper and the demonstration of incorporating this in SNR calculations should enable the selection of pixel size to be optimal.

The system designer may have some control over D (image diameter) by telescope specification and by site selection, however, usually the atmosphere results in a range of D. Figures 10 through 18 demonstrate that it may be better to maximize the SNR for small D by selecting a small pixel size, and then be penalized when the "seeing" is bad (D increases), rather than selecting a large pixel size and always have low SNR.

Figures 10 through 18 give a concrete illustration of how the correct pixel size can be selected, what SNR will result, and if the optimal pixel size cannot be selected (due to practical constraints) what penalty will be paid in SNR. In addition, it will be evident that the electro-optical system will provide sufficient or insufficient SNR for the detection system, human or electronic.

REFERENCES

1. K. Seyrafi, "Electro-optical Systems Analysis", Electro-Optical Research Company Publication, Los Angeles, CA, 1973.

2. R. Weber, "Visual Magnitude Flux Rate Density Standards for Sunlight Incident on Photoemissive Surfaces", Technical Note 1974-20, Lincoln Laboratory, M.I.T., (6 May 1974) DDC AD-779822/6.

3. A. Papoulis, "Probability, Random Variables, and Stochastic Processes" (McGraw-Hill, New York, 1965), P 139.

4. Seyrafi, P 269.

5. G. J. Mayer and M. J. MacDonald, "Parallel Signal Processing for Optical Satellite Detection", Real-Time Signal Processing IV, Proc. SPIE, 298, 173-183 (1982).

ACKNOWLEDGMENT

When Robert Weber reviews a paper he considers the technical and the grammatical details, and the overall clarity of the presentation. I wish to thank him for the time and effort he spent in reviewing this paper, and the numerous improvements he suggested.

I would like to thank Lynne Perry for the careful technical typing of this report.

UNCLASSIFIED

SECURITY CLASSIFICATION OF THIS PAGE *(When Data Entered)*

REPORT DOCUMENTATION PAGE		READ INSTRUCTIONS BEFORE COMPLETING FORM
1. REPORT NUMBER ESD-TR-83-245	2. GOVT ACCESSION NO. AD-A139784	3. RECIPIENT'S CATALOG NUMBER
4. TITLE *(and Subtitle)* Expected Energy Method for Electro-Optical SNR Calculations		5. TYPE OF REPORT & PERIOD COVERED Technical Report 6. PERFORMING ORG. REPORT NUMBER Technical Report 634
7. AUTHOR(s) Gerard J. Mayer		8. CONTRACT OR GRANT NUMBER(s) F19628-80-C-0002
9. PERFORMING ORGANIZATION NAME AND ADDRESS Lincoln Laboratory, M.I.T. P.O. Box 73 Lexington, MA 02173-0073		10. PROGRAM ELEMENT, PROJECT, TASK AREA & WORK UNIT NUMBERS Program Element Nos. 63428F and 12424F Project Nos. 2698 and 2295
11. CONTROLLING OFFICE NAME AND ADDRESS Air Force Systems Command, USAF Andrews AFB Washington, DC 20331		12. REPORT DATE 2 February 1984 13. NUMBER OF PAGES 44
14. MONITORING AGENCY NAME & ADDRESS *(if different from Controlling Office)* Electronic Systems Division Hanscom AFB, MA 01731		15. SECURITY CLASS. *(of this report)* Unclassified 15a. DECLASSIFICATION DOWNGRADING SCHEDULE

16. DISTRIBUTION STATEMENT *(of this Report)*

Approved for public release; distribution unlimited.

17. DISTRIBUTION STATEMENT *(of the abstract entered in Block 20, if different from Report)*

18. SUPPLEMENTARY NOTES

None

19. KEY WORDS *(Continue on reverse side if necessary and identify by block number)*

detection therory	image processing
electro-optical	pixel
SNR calculation	point source target

20. ABSTRACT *(Continue on reverse side if necessary and identify by block number)*

A mathematically robust method is derived that allows the SNR of an electro-optical system to be estimated when a point source image falls onto a sensor array of discrete picture elements (pixel). The derivation is based on a geometrical analysis of image and sensor element configuration. This method allows the optimal pixel size to be selected to maximize the expected SNR for any point source image once it's diameter is known. In this report the method is used to determine the probability of an image falling into one, two, . . . , six pixels as a function of image diameter and pixel size, and the corresponding expected maximum signal. Examples are given using this method to estimate the SNR for an electro-optical system.

DD FORM 1 Jan 73 1473 EDITION OF 1 NOV 65 IS OBSOLETE

UNCLASSIFIED

SECURITY CLASSIFICATION OF THIS PAGE *(When Data Entered)*